Effects of post-treatment method and Na co-cation on the hydrothermal stability of Cu–SSZ-13 catalyst for the selective catalytic reduction of NO_x with NH_3

Lijuan Xie [a], Fudong Liu [a,1], Xiaoyan Shi [a], Feng-Shou Xiao [b], Hong He [a,*]

[a] State Key Joint Laboratory of Environment Simulation and Pollution Control, Research Center for Eco-Environmental Sciences, Chinese Academy of Sciences, Beijing 100085, China
[b] Department of Chemistry, Zhejiang University, Hangzhou 310028, China

ABSTRACT

Post-treatment with dilute HNO_3 solution after one-pot synthesis was an effective method to prepare excellent Cu–SSZ-13 catalysts for the selective catalytic reduction of NO_x with NH_3 (NH_3–SCR). Using solutions with varying levels of acidity, catalysts with different Cu and Na contents were obtained, and the $Cu_{3.9}Na_{0.8}$–SSZ-13 catalyst showed the optimal NH_3–SCR activity and hydrothermal stability. As co-cations, Na^+ ions affected the hydrothermal stability of the one-pot-synthesized Cu–SSZ-13 catalysts greatly. Poorer hydrothermal stability was observed for catalysts with higher Na^+ contents. The results of ^{27}Al and ^{29}Si NMR spectra proved that Na^+ ions did not influence the Si(nAl) distributions in the catalysts significantly. However, H_2–TPR profiles indicated that excess Na^+ ions in the catalysts decreased the stability of Cu species seriously. Thus, poor stability of Cu species caused by excess Na^+ ions was the direct reason for the poor hydrothermal stability of the catalysts. Because of the negative effect on hydrothermal stability, excess Na^+ ions should be avoided in Cu–SSZ-13 catalysts prepared by the one-pot synthesis method.

1. Introduction

The combustion of fossil fuels in mobile power sources gives rise to nitrogen oxides (NO_x), which are serious air pollutants. The three-way catalyst (TWC) is effective at removing hydrocarbons (HC), carbon monoxide (CO) and NO_x simultaneously in gasoline engine exhaust [1,2]. Because the TWC is not effective for the removal of NO_x from diesel engine exhaust under oxygen-rich conditions, various catalyst systems for lean NO_x purification have been developed, such as lean NO_x trap (LNT) technology and selective catalytic reduction (SCR) of NO_x with reducing agents (*e.g.*, NH_3, urea, hydrocarbons) [3,4]. NH_3–SCR is a well-established approach to remove NO_x from diesel engine emission, using V_2O_5–WO_3/TiO_2 or V_2O_5–MoO_3/TiO_2 as typical catalysts. However, the narrow operation temperature window, high activity for oxidation of SO_2 to SO_3, formation of N_2O at high temperatures and the toxicity of active vanadium species limit the practical application of V-based catalysts for diesel vehicles [5–7]. Recently, metal-exchanged zeolite catalysts were reported as potential V-free catalysts for the NH_3–SCR process of diesel vehicles. From the perspective of zeolites, some large and medium pore zeolites have received much attention in the past two decades, such as Y (FAU framework), Beta (BEA framework), and ZSM-5 (MFI framework). Cu and Fe have been the most widely used transition metal ions in NH_3–SCR zeolite catalysts, owing to their good redox capacity [8,9]. Most of these catalysts show good NH_3–SCR performance under high gas hourly space velocity (GHSV), which is crucial for their practical application in diesel vehicles with limited installation space on board [10–12]. Nowadays, diesel particulate filters (DPF) are widely used in diesel particulate emission control, and are often used in upstream of the SCR catalyst. The regeneration of DPF always exposes the SCR catalysts to high temperatures (>650 °C) with high moisture [13]. Thus, high hydrothermal stability is necessary for NH_3–SCR catalysts. However, the ion-exchanged zeolite catalysts described above could not maintain good performance after hydrothermal aging treatment [14,15]. This weakness prevents those catalysts from being commercialized in real world applications.

* Corresponding author. Tel : +86 10 62849123; fax: +86 10 62849123.
E-mail address: honghe@rcees.ac.cn (H. He).
1 Present address: Materials Sciences Division, Lawrence Berkeley National Laboratory, 1Cyclotron Road, Berkeley, CA 94,720, United States.

Recently, the Cu–SSZ-13 catalyst with the chabazite (CHA) structure attracted much attention for NO_x removal from diesel engine exhaust due to its excellent performance, hydrothermal stability and high resistance to small hydrocarbon molecules in the NH_3–SCR reaction [16–20]. However, the template N,N,N-trimethyl-1-adamantammonium hydroxide (TMAdaOH) was needed in the synthesis of SSZ-13 zeolite, resulting in high cost for conventional Cu–SSZ-13 catalysts [21]. The one-pot synthesis method using copper–tetraethylenepentamine (Cu–TEPA) as a novel directing template decreased the synthesis cost greatly, which is beneficial for the wide use of Cu–SSZ-13 catalyst in industry [22]. Because the Cu loading in the initial Cu–SSZ-13 product resulting from one-pot synthesis was relatively high, a large amount of CuO formed in the untreated catalyst after direct calcination. Thus, a post-treatment procedure was necessary to adjust the Cu loading before calcination. It has been reported in our previous work that ion-exchange by NH_4NO_3 solution was effective in optimizing the Cu loading. The optimal $Cu_{3.8}$–SSZ-13 catalyst showed very good NH_3–SCR performance in the whole operation temperature range [23]. However, large amount of NH_4NO_3 was used with this method, and the wastewater from the process is aggravating the eutrophication of the aquatic environment. In this study, a new post-treatment method with dilute HNO_3 solution was developed. Compared with the use of NH_4NO_3, this new method reduced the nitrogen-containing pollutants in wastewater greatly. The experimental results also proved that this new post-treatment method is also an effective way to prepare catalysts with better NH_3–SCR performance.

As co-cations in zeolites, Na^+ ions often influence the properties of active species and the zeolite support. Torre-Abreu et al. reported that Cu species were more easily reduced in Na^+-form Cu–MOR catalysts than H^+-form [24]. Sultana et al. reported that a higher amount of Cu^+ species was present in the Na^+ form of ZSM-5 than in H^+-form ZSM-5, which could activate oxygen relatively easily [12]. They also reported a promoting effect of Na^+ ions on the retardation of coke formation on Cu–ZSM-5 catalyst [25]. Feng and Hall [26] prepared Fe–ZSM-5 catalyst free of Brønsted acid with the ratio of (Na + Fe)/Al at ca. 1. The catalyst showed much improved hydrothermal stability, and did not show deactivation on aging in wet exhaust gas up to 800 °C [26]. In this study, a relatively large amount of NaOH was used in the synthesis procedure of the initial Cu–SSZ-13 sample, and some Na^+ ions always remained in the catalyst even after post-treatment. However, the effects of the residual Na^+ ions on the NH_3–SCR performance and hydrothermal stability of this type of catalyst are still unclear. Thus, Cu–SSZ-13 catalysts with different Na^+ contents were prepared in this study, and the results indicated that the catalysts with higher Na^+ content showed poorer hydrothermal stability. Therefore, excess Na^+ ions remaining in the catalyst should be avoided in the preparation of Cu–SSZ-13 by the one-pot synthesis method.

2. Experimental

2.1. Catalyst preparation

The initial Cu–SSZ-13 sample was prepared using the method reported previously [23]. In order to obtain suitable Cu loadings in the final catalyst, post-treatment with dilute HNO_3 solution was used in this study. A suspension containing the initial sample and dilute HNO_3 solution (pH 0, 1, 2, 4) was treated at 80 °C for 12 h. Then, all samples were filtered and washed with distilled water, and dried at 100 °C overnight. Finally, the exchanged samples were calcined at 600 °C with a ramp rate of 1 °C/min to remove residual templates. According to the results of ICP, all catalysts obtained above were denoted as Cu_xNa_y–SSZ-13, where "x" and "y"

represent the Cu content and Na content in the catalyst by weight, respectively.

In order to investigate the effect of Na^+ ions on NH_3–SCR performance over Cu–SSZ-13 catalyst prepared by the one-pot synthesis method, catalysts with the same Cu content and different Na contents were also prepared. The preparation procedure was as described below. The initial Cu–SSZ-13 sample was treated by 1 mol/L $NaNO_3$ solution at pH 1 (adjusted using HNO_3 solution) at 80 °C for 12 h. After the same procedure of washing and desiccation described above, half of the obtained sample was calcined directly, and the rest sample was stirred in 1 mol/L $NaNO_3$ solution once more at 80 °C for 12 h before calcination. The calcination procedure and naming method for the two samples were the same as those described above.

In the hydrothermal aging studies, all catalysts were treated in flowing gas composed of air with 10 vol.% H_2O at 750 °C for 16 h.

2.2. NH_3–SCR activity test

The reaction conditions of SCR activity tests were controlled as follows: 500 ppm NO, 500 ppm NH_3, 5 vol.% O_2, 5 vol.% H_2O (when used), balance N_2, and 500 mL/min total flow rate. Catalyst samples (~50 mg) of 40–60 mesh size were used with gas hourly space velocity (GHSV) estimated as 400,000 h^{-1}. The effluent gas was continuously analyzed by an online NEXUS 670-FTIR spectrometer equipped with a heated, low volume (0.2 L) multiple-path gas cell (2 m). The FTIR spectra were collected throughout and the results were recorded when the SCR reaction reached a steady state. The NO_x conversion and N_2 selectivity were calculated as follows:

$$NO_x \text{ conversion} = (1 - \frac{[NO]_{out} + [NO_2]_{out}}{[NO]_{in} + [NO_2]_{in}}) \times 100\%$$

$$N_2 \text{ selectivity} = \frac{[NO]_{in} + [NH_3]_{in} - [NO_2]_{out} - 2[N_2O]_{out}}{[NO]_{in} + [NH_3]_{in}} \times 100\%$$

2.3. Catalyst characterization

The Cu contents of the catalysts were analyzed using an inductively coupled plasma instrument (OPTMIA 2000DV) with a radial view of the plasma. All samples were dissolved using strong acid solution before testing. The calibration solution was prepared using pure materials. The average of three atomic emission lines was used to determine the Cu contents in the catalysts.

Powder X-ray diffraction (XRD) measurements were carried out on a computerized PANalytical X'Pert Pro diffractometer with Cu $K\alpha$ ($\lambda = 0.15406$ nm) radiation. The data of 2θ from 5 to 40° were collected with the step size of 0.02°.

The H_2–TPR experiments were carried out on a Micromeritics AutoChem 2920 chemisorption analyzer. The samples (50 mg) were placed in a quartz reactor and were pretreated at 500 °C in a flow of air (50 mL/min) for 1 h, then cooled down to room temperature. Then H_2–TPR was performed in 10 vol.% H_2/Ar gas flow of 50 mL/min at a heating rate of 10 °C/min.

Solid state ^{29}Si and ^{27}Al MAS NMR spectra were collected on a Bruker AVANCE III 400 MHz WB Solid–State NMR spectrometer operating at the spectral frequency of 79.52 MHz (Si) or 104.29 MHz (Al). A relaxation delay of 6 s for Si and 1 s for Al was applied to collect single pulse spectra. All measurements were performed at room temperature, and TMS and $Al(NO_3)_3$ were used as external references, respectively.

Table 1
Physicochemical characterization of the catalysts obtained from different post-treatments.

	Without pretreatment	pH 4	pH 2	pH 1	pH 0
Relative crystallinity (%)	100	100	95.4	82.2	26.9
Si/Al$_2$	8.3	8.3	8.3	10.4	23.4
Cu contents (wt.%)	10.3	5.3	4.3	3.9	1.7
Na contents (wt.%)	4.6	3.7	2.5	0.8	0.7

3. Results and discussion

3.1. Characteristics of Cu$_x$Na$_y$–SSZ-13 catalysts

All four catalysts exhibited the typical diffraction peaks of the CHA zeolite structure ($2\theta = 9.5$, 14.0, 16.1, 17.8, 20.7 and 25.0°) after post-treatment with dilute HNO$_3$ solution adjusted to different pH values (Fig. S1) [27]. In order to confirm the effect of acid treatment on the catalyst structure, the relative crystallinity was calculated through comparison of peak intensity changes at $2\theta = 9.4$, 20.5 and 30.4° before and after acid treatment [28]. No obvious reduction in peak intensity was observed after post-treatment by HNO$_3$ solution with pH 4 and pH 2, and the relative crystallinity maintained at *ca.* 100%. Post-treatment by HNO$_3$ solution with pH 1 and pH 0 decreased the peak intensity distinctly, giving relative crystallinity of *ca.* 82.2% and 26.9%, respectively (Table 1). Thus, post-treatment by dilute HNO$_3$ solution with pH higher than 2 did not damage the zeolite structure noticeably. Physicochemical properties of the catalyst without acid treatment were also provided, as shown in Table 1. The SiO$_2$/Al$_2$O$_3$ ratio of the catalyst was 8.3, and the metal loading was 10.3 and 4.6 wt.% for Cu and Na, respectively. When dilute HNO$_3$ solution with pH 1 or pH 0 was used, the SiO$_2$/Al$_2$O$_3$ ratio increased to 10.4 and 23.4, respectively. It was concluded that more aluminum atoms were removed by post-treatment with stronger HNO$_3$ acid solution, and more breakdown of the lattice were expected under these conditions. Besides the different SiO$_2$/Al$_2$O$_3$ ratios, the Cu and Na content in the obtained catalysts was also decreased with the decrease of pH (Table 1). Thus, the post-treatment by dilute HNO$_3$ solution was an effective method to prepare Cu–SSZ-13 catalysts with different SiO$_2$/Al$_2$O$_3$ ratios and different metal loadings.

3.2. NH$_3$–SCR performance and hydrothermal stability of Cu$_x$Na$_y$–SSZ-13 catalysts

The NO$_x$ conversion as a function of reaction temperature between 150 and 550 °C over Cu$_x$Na$_y$-SSZ-13 catalysts at relatively high GHSV (400,000 h^{-1}) is shown in Fig. 1. As the provider of active sites, the Cu loading in the catalysts could affect the NH$_3$–SCR performance greatly. Due to its low Cu loading, the Cu$_{1.7}$Na$_{0.7}$–SSZ-13 catalyst did not show very good NH$_3$–SCR performance in over the studied temperature range. With the increase of Cu loading from 1.7 wt.% to 4.3 wt.%, the NO$_x$ conversion was improved significantly, especially in the low temperature range. However, the NO$_x$ conversion in the high temperature range (>400 °C) decreased distinctly when Cu loading was raised to 5.3 wt.% (only 57% at 550 °C), which should be related to the unselective oxidation of NH$_3$ in the high temperature range. Although different levels of NO$_x$ conversion were observed, excellent N$_2$ selectivity could be obtained for all catalysts, which was nearly 100% over the whole temperature range (Fig. S2). Compared with the others, the Cu$_{3.9}$Na$_{0.8}$–SSZ-13 and Cu$_{4.3}$Na$_{2.5}$–SSZ-13 catalysts showed the best NH$_3$–SCR performance, maintaining NO$_x$ conversion higher than 90% from 200 to 500 °C. Thus, Cu loading at *ca.* 4.0 wt.% was suitable for Cu–SSZ-13 catalysts prepared by the one-pot synthesis method.
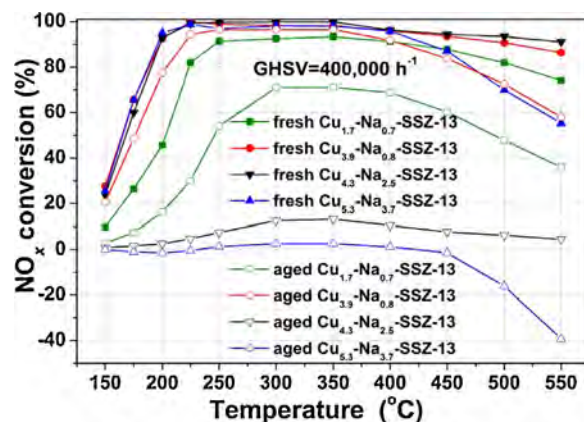

Fig. 1. NH$_3$–SCR performance of fresh (solid symbol) and aged Cu$_x$Na$_y$–SSZ-13 catalysts (hollow symbol).
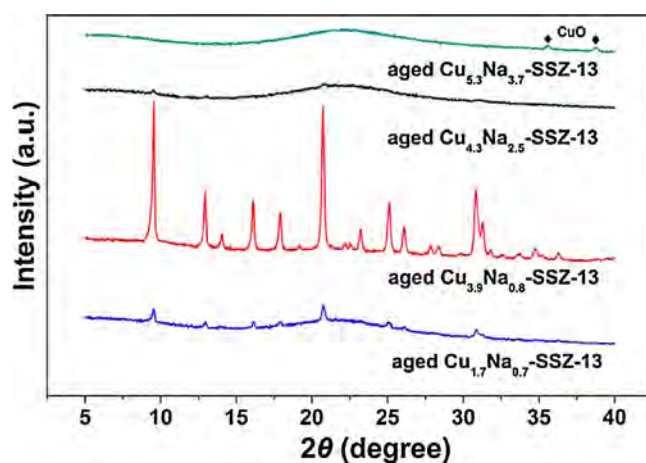

Fig. 2. XRD profiles of Cu$_x$Na$_y$–SSZ-13 catalysts after hydrothermal aging at 750 °C for 16 h.

In order to probe the hydrothermal stability, the above-mentioned four catalysts were further treated in air with 10 vol.% H$_2$O at 750 °C for 16 h. The NH$_3$–SCR activity of the aged catalysts is also shown in Fig. 1. The aged Cu$_{5.3}$Na$_{3.7}$–SSZ-13 and Cu$_{4.3}$Na$_{2.5}$–SSZ-13 catalysts almost lost their NH$_3$–SCR activity completely, while Cu$_{1.7}$Na$_{0.7}$–SSZ-13 and Cu$_{3.9}$Na$_{0.8}$–SSZ-13 catalysts exhibited better hydrothermal stability. Importantly, the aged Cu$_{3.9}$Na$_{0.8}$–SSZ-13 catalyst showed the best hydrothermal stability, with NO$_x$ conversion higher than 80% from 200 to 450 °C. Therefore, the post-treatment by dilute HNO$_3$ solution with pH 1 was the optimal procedure to prepare the catalyst with both excellent NH$_3$–SCR performance and high hydrothermal stability. The NH$_3$–SCR performance of fresh Cu$_{3.9}$Na$_{0.8}$–SSZ-13 catalyst was also tested under the simulated condition with water, as shown in Table 2. The presence of 5 vol.% H$_2$O decreased the NO$_x$ conversion at low temperatures (<200 °C) mainly due to the competitive adsorption by H$_2$O adsorption, and increased the NO$_x$ conversion at high temperatures (>400 °C) probably due to the inhibition effect of H$_2$O on the unselective catalytic oxidation of NH$_3$ [23]. Nevertheless, the NO$_x$ conversion maintained nearly 100% from 225 to 550 °C, indicating the catalyst also do well under the condition with water.

In order to evaluate the degradation of the zeolite structure caused by the hydrothermal aging, XRD measurements were performed for the aged catalysts, as shown in Fig. 2. The aged Cu$_{4.3}$Na$_{2.5}$–SSZ-13 and Cu$_{5.3}$Na$_{3.7}$–SSZ-13 catalysts showed complete collapse of the zeolite structure, with a broad feature representing an amorphous phase, which was consistent with their

Table 2
NH$_3$–SCR performance of Cu$_{3.9}$Na$_{0.8}$–SSZ-13 catalysts under simulate condition with 5% H$_2$O.

	Temperature (°C)										
	150	175	200	225	250	300	350	400	450	500	550
NO$_x$Conversion (%)	12.1	29.8	58.4	99.8	100	100	100	100	100	100	100

total loss of NH$_3$–SCR performance as described above. Some CuO was detected in the aged Cu$_{5.3}$Na$_{3.7}$–SSZ-13 catalyst. Because NH$_3$ could be over-oxidized to NO$_x$ in the presence of CuO, negative NO$_x$ conversion at high temperatures (>450 °C) was achieved for the aged Cu$_{5.3}$Na$_{3.7}$–SSZ-13 catalyst (Fig. 1). Little change was observed for the hydrothermally aged Cu$_{3.9}$Na$_{0.8}$–SSZ-13 catalyst, indicating its very good hydrothermal stability. Although the typical peaks of the CHA structure were also maintained for the aged Cu$_{1.7}$Na$_{0.7}$–SSZ-13 catalyst, the intensity of the zeolite peaks decreased significantly and an amorphous phase was apparent. It was hypothesized that the excessive dealumination of this catalyst was an important factor in its decreased hydrothermal stability.

H$_2$–TPR profiles of the four Cu$_x$Na$_y$–SSZ-13 catalysts are shown in Fig. 3. Reduction of isolated Cu^{2+} in zeolites has been proposed to follow a two-step mechanism, namely the reduction from Cu^{2+} to Cu$^+$ (at lower temperatures) and the reduction from Cu$^+$ to Cu^0 (at higher temperatures). However, the reduction of the dispersed bulk CuO to Cu^0 occurred in a single step in the low temperature range (200–300 °C) [23,29,30]. According to the profile of the fresh Cu$_{1.7}$Na$_{0.7}$–SSZ-13, Cu$_{3.9}$Na$_{0.8}$–SSZ-13 and Cu$_{4.3}$Na$_{2.5}$–SSZ-13 catalysts, the integrated area for H$_2$ consumption below 500 °C contributed *ca.* 49, 49 and 50% of the total H$_2$ consumption area, respectively. Thus, it is reasonable to conclude that only isolated Cu^{2+} was present in the above three catalysts. The peaks at 170, 222 and 345 °C could be assigned to the reduction of Cu^{2+} located in different cationic sites to Cu$^+$ [23]. The H$_2$ consumption below 400 °C for the Cu$_{5.3}$Na$_{3.7}$–SSZ-13 catalyst contributed *ca.* 61% of the total, indicating that the reduction from Cu$^+$ to Cu^0 also occurred in the low temperature range. Thus, the peak at *ca.* 207 °C was assigned to the reduction peak of highly dispersed CuO in the catalyst, although it was not observed in XRD profile. Compared with isolated Cu^{2+}, Cu^0 was found to be less efficient for SCR reactions in the low temperature range (≤200 °C) [31]. Thus, the Cu$_{5.3}$Na$_{3.7}$–SSZ-13 catalyst did not show the best deNO$_x$ efficiency although it had the highest Cu loading. It was reported that the high stability of active species is an important factor for Cu/zeolite catalysts with high hydrothermal stability, and the reduction from Cu$^+$ to Cu^0 was expected when the chabazite structure began to degrade [32,33]. Thus, isolated Cu^{2+} ions with higher reduction

temperature from Cu$^+$ to Cu^0 are expected to be more stable in the chabazite structure. The Cu$_{1.7}$Na$_{0.7}$–SSZ-13 and Cu$_{3.9}$Na$_{0.8}$–SSZ-13 catalysts showed extremely high reduction temperature for Cu$^+$ to Cu^0 reduction (at *ca.* 900 °C), which indicated the excellent stability of Cu^{2+} species in these materials. However, no Cu species with such high stability was observed in Cu$_{4.3}$Na$_{2.5}$–SSZ-13 and Cu$_{5.3}$Na$_{3.7}$–SSZ-13 catalysts. Considering these two catalysts possessed an almost intact zeolite structure (Table 1), the poor stability of Cu species should be the reason for their poor hydrothermal stability. Therefore, isolated Cu^{2+} species with extremely high thermal stability are necessary to obtain a Cu–SSZ-13 catalyst with both good NH$_3$–SCR performance and high hydrothermal stability. Based on the composition of Cu$_{4.3}$Na$_{2.5}$–SSZ-13 and Cu$_{3.9}$Na$_{0.8}$–SSZ-13 catalysts, it was hypothesized that the Na$^+$ ions in the catalysts affected their hydrothermal stability seriously, as will be discussed below in detail.

Ion exchange by NH$_4$NO$_3$ solution was also proved to be an effective post-treatment method to prepare Cu–SSZ-13 catalyst, and the optimal Cu$_{3.8}$Na$_{1.2}$–SSZ-13 catalyst showed very good NH$_3$–SCR activity [23]. In order to compare the two catalysts obtained by different methods, the turn-over frequency (TOF) of NO$_x$ over Cu species at 150 °C was calculated, where the NO$_x$ conversion was less than 40% [34]. Assuming that all Cu species were active in the studied catalysts, the TOF was defined as the number of NO$_x$ molecules converted per Cu per second. Although the two catalysts contained nearly equal amounts of Cu, their NH$_3$–SCR performance was quite different. Not only did the fresh Cu$_{3.9}$Na$_{0.8}$–SSZ-13 catalyst show higher TOF (1.69×10^{-3} s^{-1}) than the fresh Cu$_{3.8}$Na$_{1.2}$–SSZ-13 catalyst (0.84×10^{-3} s^{-1}), the aged Cu$_{3.9}$Na$_{0.8}$–SSZ-13 catalyst also showed higher TOF (1.26×10^{-3} s^{-1}) than the aged Cu$_{3.8}$Na$_{1.2}$–SSZ-13 catalyst (0.64×10^{-3} s^{-1}). Therefore, post-treatment by dilute HNO$_3$ solution was better than the procedure using NH$_4$NO$_3$ solution to prepare a catalyst with excellent NH$_3$–SCR activity and hydrothermal stability.

3.3. Influence of Na$^+$ on NH$_3$–SCR performance of Cu$_{3.9}$Na$_x$–SSZ-13 catalysts

Three catalysts with the same Cu content and different Na$^+$ contents were prepared in this study, which were denoted as Cu$_{3.9}$Na$_{0.8}$–SSZ-13, Cu$_{3.9}$Na$_{1.7}$–SSZ-13 and Cu$_{3.9}$Na$_{2.2}$–SSZ-13 on the basis of elemental analysis results. The NH$_3$–SCR performance of the fresh and aged catalysts is shown in Fig. 4. With the increase of Na$^+$ content in the catalysts, only a small decrease of NO$_x$ conversion was observed for the fresh catalysts. However, after hydrothermal treatment in air with 10 vol.% H$_2$O at 750 °C for 16 h, the NO$_x$ conversion decreased greatly along with the increase of Na content. When the Na$^+$ content increased from 0.8 to 1.7 wt.%, the NO$_x$ conversion decreased greatly. If more Na$^+$ ions were loaded (*ca.* 2.2 wt.%), the catalyst became almost completely inactive for NH$_3$–SCR reaction. The above results indicated that the presence of excess Na$^+$ ions in the catalyst could severely decrease the hydrothermal stability of the Cu–SSZ-13 catalyst prepared by the one-pot synthesis method.

The XRD profiles of the aged Cu$_{3.9}$Na$_x$–SSZ-13 catalysts are shown in Fig. 5. Compared with the aged Cu$_{3.9}$Na$_{0.8}$–SSZ-13 catalyst, the peak intensity of the chabazite structure decreased greatly accompanied by the appearance of amorphous phase for the aged
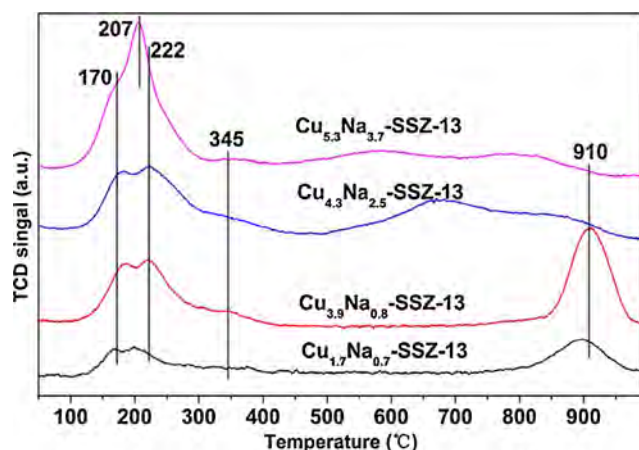

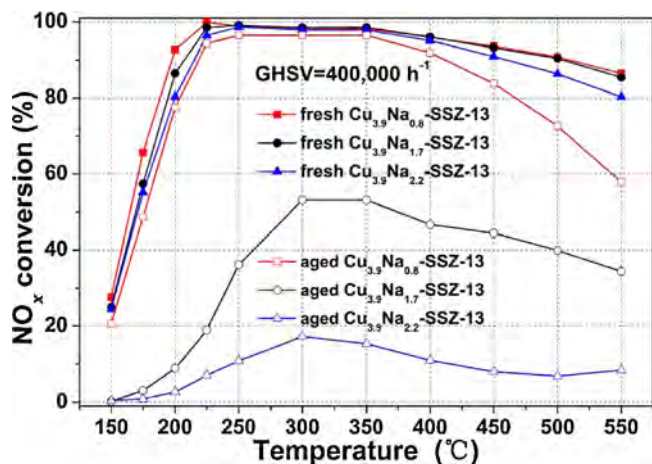**Fig. 3.** H$_2$–TPR profiles of Cu$_x$Na$_y$–SSZ-13 catalysts.

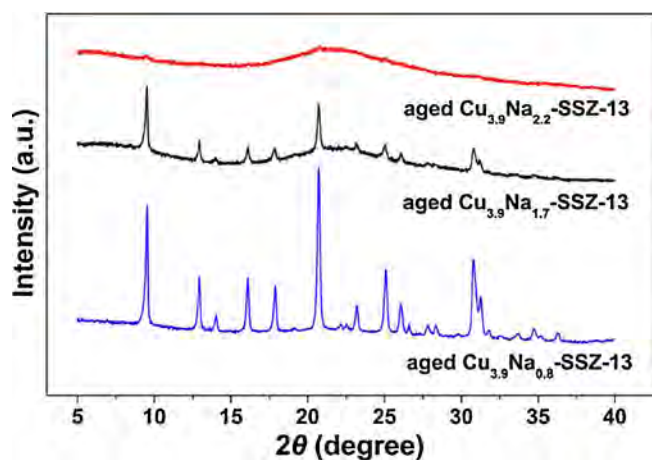**Fig. 4.** NH_3–SCR performance of fresh (solid symbol) and aged $Cu_{3.9}Na_x$–SSZ-13 catalysts (hollow symbol).

Fig. 5. XRD profiles of $Cu_{3.9}Na_x$–SSZ-13 catalysts after hydrothermal aging at 750 °C for 16 h.

$Cu_{3.9}Na_{1.7}$–SSZ-13 catalyst. Even more seriously, the CHA structure disappeared completely for the aged $Cu_{3.9}Na_{2.2}$–SSZ-13 catalyst with the highest Na^+ content. It is well known that a catalyst having more breakdown of the zeolite lattice structure or more unstable active species are more easily inactivated by hydrothermal treatment. Therefore, the effects of Na^+ ions on the zeolite framework and the Cu species will be discussed below.

Solid state NMR experiments were carried out to characterize the framework of the $Cu_{3.9}Na_x$–SSZ-13 catalysts. ^{27}Al solid state NMR results can provide information about the structural environment of Al atoms in zeolites. The Al atom in the framework has 4-fold coordination (Al^{IV}), which presents a typical chemical shift of 50–60 ppm. However, if the Al atom is removed from the zeolite framework, the Al atom can be located outside the lattice, showing a 6-fold-type coordination (Al^{VI}) with a 0–10 ppm chemical shift in ^{27}Al NMR spectra [35,36]. As shown in Fig. 6(A), a small amount of Al^{VI} atoms were detected for the $Cu_{3.9}Na_{0.8}$–SSZ-13 catalyst, while

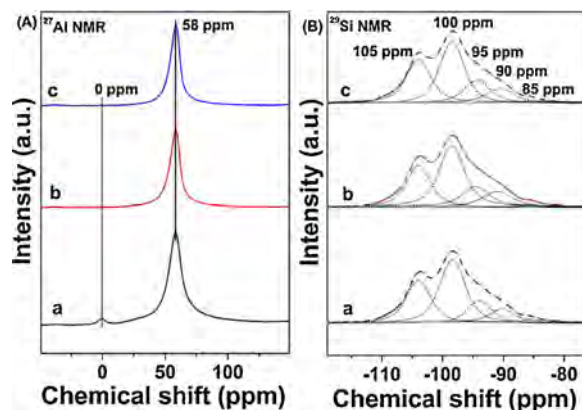**Fig. 6.** Solid state ^{27}Al and ^{29}Si NMR spectra of $Cu_{3.9}Na_x$–SSZ-13 catalysts: (a) $Cu_{3.9}Na_{0.8}$–SSZ-13; (b) $Cu_{3.9}Na_{1.7}$–SSZ-13; (c) $Cu_{3.9}Na_{2.2}$–SSZ-13.

only Al^{IV} atoms existed in $Cu_{3.9}Na_{1.7}$–SSZ-13 and $Cu_{3.9}Na_{2.2}$–SSZ-13 catalysts. According to the results of ICP analysis, the bulk SiO_2/Al_2O_3 ratio was 10.4, 12.8 and 12.4 for $Cu_{3.9}Na_{0.8}$–SSZ-13, $Cu_{3.9}Na_{1.7}$–SSZ-13 and $Cu_{3.9}Na_{2.2}$–SSZ-13 catalysts, respectively. Compared with the bulk SiO_2/Al_2O_3 ratio of the initial Cu–SSZ-13 sample, the SiO_2/Al_2O_3 ratios of all these catalysts were improved to a certain extent. This was direct evidence that dealumination occurred for all the three catalysts, although no evidence of Al^{VI} atoms was observed in the two catalysts with higher Na^+ content. Because much more $NaNO_3$ (1 mol/L) was added in the preparation procedure of $Cu_{3.9}Na_{1.7}$–SSZ-13 and $Cu_{3.9}Na_{2.2}$–SSZ-13 catalysts, it was thought that the Al^{3+} (Al^{VI}) caused by dealumination was removed along with NO_3^- in the washing process. Thus, ^{27}Al solid state NMR results did not clearly indicate whether or not the Na^+ ions affected the zeolite framework in the post-treatment process, and more characterization was necessary to answer this question.

^{29}Si solid state NMR spectra could give relevant information about the arrangement of Si and Al atoms in the framework. The application of this technology is based on the fact that the ^{29}Si chemical shift is very sensitive to its environment, in other words, the number of aluminum–oxygen tetrahedra connected to each silicon-oxygen tetrahedron (Si(nAl)). The framework SiO_2/Al_2O_3 ratio could be calculated using the areas of different Si(nAl) by the following equation [36,37]:

$$Si/Al = \frac{\sum_{n=0}^{4} Isi(Al)}{\sum_{n=0}^{4} 0.25n Isi(Al)}$$

The advantage of this calculation method is that the effect of extra-framework aluminum is eliminated, and the results can represent the stability of a zeolite better than the bulk SiO_2/Al_2O_3 ratio. Fig. 6(B) shows the ^{29}Si solid state NMR spectra and the optimal deconvolution of the relevant peaks corresponding to $Cu_{3.9}Na_x$–SSZ-13 catalysts. The five signals at *ca.* −85, −90, −95, −100 and −105 ppm correspond to distinct Si(4Al), Si(3Al), Si(2Al),

Table 3
Calculated areas of the different types of Si(nAl) signals from deconvolution of ^{29}Si NMR spectra for $Cu_{3.9}Na_x$–SSZ-13 catalysts.

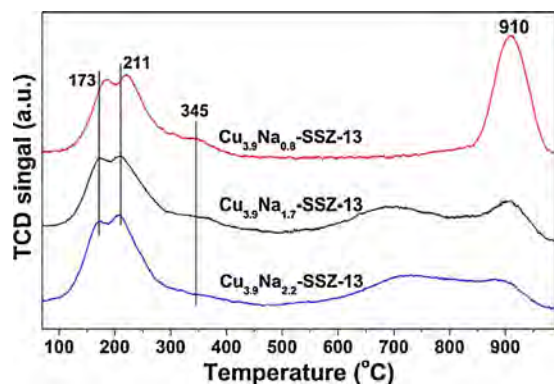| Catalysts	Areas for the different types of Q^4(nAl) signals					FrameworkSiO_2/Al_2O_3
	Si(4Al)	Si(3Al)	Si(2Al)	Si(1Al)	Si(0Al)	
$Cu_{3.9}Na_{0.8}$–SSZ-13	1.2	8.69	15.48	45.06	29.57	7.48
$Cu_{3.9}Na_{1.7}$–SSZ-13	1.05	11.95	14.18	43.71	29.11	7.14
$Cu_{3.9}Na_{2.2}$–SSZ-13	1.14	10.22	16.03	42.87	29.74	7.26

Fig. 7. H_2–TPR profiles of $Cu_{3.9}Na_x$–SSZ-13 catalysts.

Si(1Al) and Si(0Al), respectively [38]. The area of each peak was calculated, as shown in Table 3. No obvious change in the distribution of Si(nAl) was observed for $Cu_{3.9}Na_x$–SSZ-13 catalysts. The $Cu_{3.9}Na_x$–SSZ-13 catalysts retained almost the same zeolite structure even though the treatment procedures were greatly different. Therefore, the damage of the zeolite structure was mainly caused by the acid solution, and the presence of Na^+ ions was irrelevant.

H_2–TPR experiments were carried out to study the influence of Na^+ ions on Cu species, and the results are shown in Fig. 7. As stated above, the reduction temperature and reduction process of different Cu species (such as CuO, Cu^{2+}, Cu^+) was different form each other. The ratio of the integrated area for H_2 consumption at the low temperatures was effective to describe the state of Cu species. According to the calculation, the integrated area for H_2 consumption below 500 °C of $Cu_{3.9}Na_{0.8}$–SSZ-13, $Cu_{3.9}Na_{1.7}$–SSZ-13 and $Cu_{3.9}Na_{2.2}$–SSZ-13 contributed *ca.* 49, 51 and 50% of the total H_2 consumption area, respectively. Thus, all Cu species should be isolate Cu^{2+} in the three catalysts. The three reduction peaks in the low temperature range (*ca.* 173, 211 and 345 °C) were assigned to the reduction of isolated Cu^{2+} to Cu^+. In our previous report, EPR and H_2–TPR tests were both carried out to assign the local structure of Cu species together, and the H_2 reduction peaks at 179, 247, and 329 °C for Cu–SSZ-13 catalyst were attributed to isolated Cu^{2+} ions locating in three different sites of chabizite structure (site IV, I, and III), respectively [23]. In this study, the H_2 reduction peaks of the three catalysts were similar to that observed in the previous paper. Thus, it was reasonable to conclude that the isolated Cu^{2+} also located in these three different sites. The previous studies reported that the alkali cations could lower the reduction temperature of Cu species [12]. In the present study, the reduction peaks moved to lower temperature by *ca.* 10 °C with the increase of Na^+ content. Though the difference was not obvious in the low temperature range, a significant difference was observed in the high temperature range, where the reduction from Cu^+ to Cu^0 occurred. The ratio of Cu species with extremely high stability (*ca.* 900 °C) dropped significantly with the increase of Na^+ content, indicating that the excess Na^+ was not beneficial for the stability of active species in the Cu–SSZ-13 catalysts prepared by the one-pot synthesis method. Migration of Cu species to less stable state and aggregation to CuO more likely happened with a higher Na content in the catalyst during the hydrothermal treatment process, which should be related to the decreased stability of active species (Fig. S3). The detrimental effect of Na ions on hydrothermal stability of the catalyst was reflected through its effect on Cu species. The decreasing trend in the stability of Cu species was consistent with the poor NH_3–SCR performance as described above for the aged $Cu_{3.9}Na_x$–SSZ-13 catalysts. Therefore, considering the effects of Na^+ ions on the zeolite structure, it was concluded clearly that decreased stability of Cu species resulting from excess Na^+ ions was

the direct reason leading to the poor hydrothermal stability of the Cu–SSZ-13 catalysts prepared by the one-pot synthesis method.

4. Conclusions

The post-treatment by dilute HNO_3 solution was an effective method to adjust the Cu and Na contents in the Cu–SSZ-13 catalyst prepared by one-pot synthesis method. The optimal $Cu_{3.9}Na_{0.8}$–SSZ-13 catalyst obtained from the post-treatment by dilute HNO_3 solution with pH 1 showed the best NH_3–SCR activity and hydrothermal stability. As co-cation, Na^+ ions affected the hydrothermal stability of the one-pot-synthesized Cu–SSZ-13 catalysts greatly. The catalysts with higher Na^+ content showed poorer hydrothermal stability. The results of ^{27}Al and ^{29}Si NMR spectra indicated that the catalysts with different Na^+ contents possessed almost the same zeolite structure. However, the H_2–TPR results illustrated that the stability of Cu species decreased seriously along with the increase of Na^+ ions in the catalysts. Thus, the Cu species with poor stability aroused by high Na^+ content resulted in the poor hydrothermal stability of the catalysts. Therefore, it is better to precisely control the amount of Na^+ ions maintained in Cu–SSZ-13 catalysts prepared by one-pot synthesis method to obtain the excellent NH_3–SCR performance and hydrothermal stability simultaneously.

Appendix A. Supplementary data

Supplementary data associated with this article can be found, in the online version, at http://dx.doi.org/10.1016/j.apcatb.2015.05.032

References

[1] P. Granger, V.I. Parvulescu, Chem. Rev. 111 (2011) 3155–3207.
[2] Z. Liu, S. Ihl Woo, Catal. Rev. 48 (2006) 43–89.
[3] W.S. Epling, L.E. Campbell, A. Yezerets, N.W. Currier, J.E. Parks, Catal. Rev. 46 (2004) 163–245.
[4] B. Sandro, K. Oliver, T. Arno, A. Roderik, Catal. Rev. 50 (2008) 492–531.
[5] J.P. Dunn, P.R. Koppula, H.G. Stenger, I.E. Wachs, Appl. Catal. B 19 (1998) 103–117.
[6] J. Li, H. Chang, L. Ma, J. Hao, R.T. Yang, Catal. Today 175 (2011) 147–156.
[7] M. Yates, J.A. Martín, M.Á. Martín-Luengo, S. Suárez, J. Blanco, Catal. Today 107–108 (2005) 120–125.
[8] M. Colombo, I. Nova, E. Tronconi, Appl. Catal. B 111–112 (2012) 433–444.
[9] H. Sjövall, R.J. Blint, L. Olsson, Appl. Catal. B 92 (2009) 138–153.
[10] C. He, Y. Wang, Y. Cheng, C.K. Lambert, R.T. Yang, Appl. Catal. A 368 (2009) 121–126.
[11] J. Li, R. Zhu, Y. Cheng, C. k. Lambert, R.T. Yang, Environ. Sci. Technol. 44 (2010) 1799–1805.
[12] A. Sultana, T. Nanba, M. Haneda, M. Sasaki, H. Hamada, Appl. Catal. B 101 (2010) 61–67.
[13] H. Zheng, J.M. Keith, Catal. Today 98 (2004) 403–412.
[14] J. Park, H. Park, J. Baik, I. Nam, C. Shin, J. Lee, B. Cho, S. Oh, J. Catal. 240 (2006) 47–57.
[15] I. Masaoki, S. Hirofumi, Chem. Commun. 47 (2011) 3966–3968.
[16] D.W. Fickel, D.A. Elizabeth, J.A. Lauterbach, R.F. Lobo, Appl. Catal. B 102 (2011) 441–448.
[17] J.H. Kwak, D. Tran, S.D. Burton, J. Szanyi, J.H. Lee, C.H.F. Peden, J. Catal. 287 (2012) 203–209.
[18] Q. Ye, L. Wang, R.T. Yang, Appl. Catal. A 427–428 (2012) 24–34.
[19] U. Deka, I. Lezcano-Gonzalez, B.M. Weckhuysen, A.M. Beale, ACS Catal. 3 (2013) 413–427.
[20] L. Ma, Y. Cheng, G. Cavataio, R.W. McCabe, L. Fu, J. Li, Appl. Catal. B 156–157 (2014) 428–437.
[21] S.I. Zones, J. Chem. Soc. Faraday Trans. 87 (1991) 3709–3716.

[22] L. Ren, L. Zhu, C. Yang, Y. Chen, Q. Sun, H. Zhang, C. Li, F. Nawaz, X. Meng, F.-S. Xiao, Chem. Commun. 47 (2011) 9789–9791.

[23] L. Xie, F. Liu, L. Ren, X. Shi, F.S. Xiao, H. He, Environ. Sci. Technol. 48 (2014) 566–572.

[24] C. Torre-Abreu, M.F. Ribeiro, C. Henriques, G. Delahayb, Appl. Catal. B 14 (1997) 261–272.

[25] A. Sultana, T. Nanba, M. Haneda, H. Hamada, Catal. Commun. 10 (2009) 1859–1863.

[26] X. Feng, W.K. Hall, J. Catal. 166 (1997) 368–376.

[27] M.M.J. Treacy, J.B. Higgins, Collection of Simulated XRD Patterns for Zeolites, 5th ed., Elsevier, Amsterdam, 2007.

[28] Y. Naoki, I. Masaya, K. Yoshimichi, I. Yusuke, S. Masahiro, S. Tsuneji, Micropor. Mesopor. Mater. 158 (2012) 141–147.

[29] M. Richter, M. Fait, R. Eckelt, M. Schneider, J. Radnik, D. Heidemann, R. Fricke, J. Catal. 245 (2007) 11–24.

[30] R. Kefirov, A. Penkova, K. Hadjiivanov, S. Dzwigaj, M. Che, Micropor. Mesopor. Mater. 116 (2008) 180–187.

[31] J. Xue, X. Wang, G. Qi, J. Wang, M. Shen, W. Li, J. Catal. 297 (2013) 56–64.

[32] F. Gao, E.D. Walter, E.M. Karp, J. Luo, R.G. Tonkyn, J.H. Kwak, J. Szanyi, C.H.F. Peden, J. Catal. 300 (2013) 20–29.

[33] A. Sultana, T. Nanba, M. Sasaki, M. Haneda, K. Suzuki, H. Hamada, Catal. Today 164 (2011) 495–499.

[34] L. Wang, W. Li, G. Qi, D. Weng, J. Catal. 289 (2012) 21–29.

[35] S. Li, S.-J. Huang, W. Shen, H. Zhang, H. Fang, A. Zheng, S.-B. Liu, F. Deng, J. Phys. Chem. C 112 (2008) 14486–14494.

[36] Y. Fan, X. Bao, X. Lin, G. Shi, H. Liu, J. Phys. Chem. B 110 (2006) 15411–15416.

[37] F. Dogan, K.D. Hammond, G.A. Tompsett, H. Huo, J.W. Curtis Conner, S.M. Auerbach, C.P. Grey, J. Am. Chem. Soc. 131 (2009) 11062–11079.

[38] P. Morales-Pacheco, F. Alvarez, L. Bucio, J.M. Domínguez, J. Phys. Chem. C 113 (2009) 2247–2255.